Measurement of L-shell X-ray production cross sections in ^{89}Y, ^{158}Gd and ^{209}Bi due to 0.3 MeV/u – 1.0 MeV/u ^{12}C ions

E.O Ejeh[a], T.T Hlatshwayo,[a] M. Madhuku[b], M Legodi[a], M. Msimanga[b,c*]

[a] Physics Department, University of Pretoria, P Bag X20, Pretoria 0002, South Africa.

[b] iThemba LABS TAMS, National Research Foundation, P Bag 11, WITS, 2050, Johannesburg, South Africa

[c] Physics Department, Tshwane University of Technology, P Bag X680, Pretoria 0001, South Africa

*Corresponding Author

Email address: MsimangaM@tut.ac.za

Abstract

Experimental heavy ion induced X–ray production cross sections in matter continue to be of importance for both fundamental ion-atom collision studies as well as practical applications such as in nuclear analytical techniques. This work presents results of L-shell X-ray production cross section measurements in ^{89}Y, ^{158}Gd and ^{209}Bi due to 4 MeV-12 MeV $^{12}C^{q+}$ projectile ions. Experimental data are compared with theoretical calculations based on the ECPSSR, ECPSSR+EC and ECPSSR-UA models. Data show fairly good, albeit energy dependent agreement with the different models for yttrium and gadolinium cross sections. For bismuth, all three models overestimate data by an almost constant factor of two. The effect of multiple ionization on the L-line intensity ratios is also presented for gadolinium and bismuth targets.

Keywords: X-ray production cross section; Heavy ion PIXE; ECPSSR theory; Multiple ionization

1. Introduction

Adequate knowledge of inner shell ionization is of primary importance basic ion-atom interaction studies and in applied nuclear techniques like Particle Induced X-ray Emission (PIXE). PIXE is a powerful, non-destructive qualitative and quantitative ion beam analysis (IBA) technique for the analysis of thin target and thick samples (Cohen, 1990; Scafes et al., 2014) . It is a widely used analytical technique in many IBA laboratories because of its sensitivity especially when analysing thin film targets. Although, the sensitivity becomes low when thick targets are analysed, it is still a fairly a good qualitative analysis method (Scafes et al., 2014). The PIXE technique makes it possible to detect many elements in a sample target at the same time in a matter of minutes. The application of PIXE in various fields such as biology, geology, environmental sciences, arts, archaeology, environmental science, bio-medical, etc, has the technique firmly established as one of the main Ion Beam Analytical (IBA) techniques (Govil, 2001). Recent research has been drawn towards the implementation of simultaneous IBA techniques for the analysis of materials. One such example involves the combination of PIXE with Secondary Ion Mass Spectroscopy (SIMS) using heavy (Z>3) projectile ions at low MeV energies (Msimanga et al., 2019; Tadić et al., 2014).

The application of PIXE using heavy ions, or HI-PIXE, for quantitative analysis requires an accurate database of heavy ion induced X-ray production cross sections (Reis and Jesus, 1996). Available literature shows that most PIXE measurements are performed using light ion beams such as protons and helium over a wide energy range (Ryan, 2011; Scafes et al., 2014). This is partly because of the availability of comprehensive databases of fundamental parameters such as X-ray production and stopping cross-sections for light ion beams. The growing research interest in HI-PIXE (Bransden et al., 1993) is because it promises to be more sensitive as heavy ions lead to larger X-ray yields than light ions when they are used as projectiles (Lapicki, 2002). Therefore, a good understanding of the ionization cross sections by heavy ions is imperative to ensure accurate data interpretation in quantitative analysis. The insufficiency of experimental data of heavy ion X-ray production cross sections is one of the major limiting factors in the wide scale implementation of HI-PIXE. Other important factors include effects of multiple ionization (MI) and the subsequent complexities of processing heavy ion spectra. In particular, there is pronounced scarcity of experimental data for heavy-ion L shell ionization cross sections when compared to proton and helium induced ionization cross section data (Msimanga et al., 2016; Orlić et al., 1998;

Prieto et al., 2017; Schmelmer et al., 2001). Over the years, different theoretical models have been developed to describe inner shell ionization processes by ions and these models have been compared to experimental ionization and X-ray production cross sections. When heavy ions (Z>2) are involved, the ionization process becomes rather complicated. Many theories founded on either the first Plane-Wave Born Approximation (PWBA) or the Semi-Classical Approximation (SCA) have been used to describe atomic collisions involving heavy ions. Of these, the most widely accepted theory that is used in IBA is ECPSSR, which is a modification of the PWBA (Brandt and Lapicki, 1981). ECPSSR theory corrects for the effects of Energy loss (E) and Coulomb deflection (C) of the incident ion, Perturbation of the Stationary States (PSS) of the atomic inner shell electrons of the target atom and the Relativistic (R) nature of the inner shell of target atom. ECPSSR predictions generally show good agreement between experiment and theory for L_1- and L_2-subshells but underestimate experiment for the L_3-subshell (Lapicki, G. McDaniel, 1980). The accuracy of the model depends on the atomic numbers of the projectile and target as well as the energy of the projectile ion. Further work on the ECPSSR theory by Sarkadi and Mukoyama that takes into account the overlaps of projectile and target atom electron orbitals resulted in the ECPSSR-United Atom (UA) model (ECPSSR-UA), which corrects for the binding energy of the target atom electrons due to the presence of the projectile (Brandt and Lapicki, 1979; Sarkadi and Mukoyama, 1991). X-ray production for medium to relatively high energy is described fairly well by the ECPSSR-UA model but there is still need for further modifications and improvement at low energies (< 1 MeV/u), particularly for intermediate to very heavy ions.

This work reports on results of measurement of new L-shell X-ray production cross sections in ^{89}Y, ^{158}Gd and ^{209}Bi due to $^{12}C^{q+}$ ions in the 4 MeV to 12 MeV energy range. Experimental data are compared to ECPSSR and ECPSSR+UA theoretical predictions calculated by the ISICSoo programme (Paul and Muhr, 1986) . Ionization collisions can either be symmetric or asymmetric. When the ratio of the projectile's atomic number Z_p to the target atomic number Z_t is far less than 1, i.e.$\frac{Z_p}{Z_t} \ll 1$, the collision is asymmetric and, in such cases, direct ionization is dominant. When the collision is symmetric (or close to symmetric), i.e. when,$\frac{Z_p}{Z_t} \lesssim 1$, the electron capture (EC) process becomes important as well (Kumar et al., 2017). The contribution of electron capture to total ionization by the projectile was also considered through ECPSSR + EC calculations using the ECRS08 code by Horvat (Horvat, 2009).

As a result of complex ion-target interactions associated with heavy ion collisions, the use of heavy ions over protons or helium ions in X-ray cross section measurements comes with additional unwanted effects (Miranda et al., 2007) that need to be corrected for to ensure proper comparison with theory. Among others, one effect that was considered in this present work is, multiple ionization (MI), which leads to shifts in characteristic X-ray energies. Multiple ionization, which is defined as production of more than one vacancy in a single collision is an important process to consider especially in heavy ion collisions. It leads to an increase in the binding energies of the target electrons and a subsequent shift in the characteristic energies. The shifts in characteristic X-ray energies in turn lead to changes in the (energy dependent) detection efficiency, so a detector efficiency correction needs to be carried out. Due to the finite thickness of the films used in this study, change in the incident beam energy due to energy loss through the film was taken into account through an energy loss correction procedure.

2. EXPERIMENTAL

Thin film samples of yttrium, gadolinium and bismuth were produced by electron beam deposition onto a mylar *(polyethylene terephtalate*) substrate. Rutherford Backscattering (RBS) analysis was used to measure the thickness of the films at the University of Pretoria (UP) Van de Graaf accelerator using 1.6 MeV helium ions. Heavy ion induced X–ray yield measurements were carried out on the microprobe beam line of the 6 MV tandem accelerator at iThemba LABS. The beam current in the microprobe chamber was kept at 0.5 nA for a total charge collection of 1.0 μC. The beam spot was deliberately de-focussed to about 2.0 mm^2 to minimize sample heating. Pressure in the target chamber during measurement was about 5 $x10^{-6}$ mbar. The X-ray spectra and the backscattered ion spectra were measured simultaneously. The X-rays were registered by a Si (Li) detector with resolution of 137 eV FWHM at 5.9 keV at an angle of 135^o from the incident beam direction. To determine the backscattered ion yield, a Canberra PIPS detector mounted at 150^o from the incident beam direction was used. The X-ray intensities and the number of backscattered incident ions were extracted from multi-peak fit analysis using Origin® software. Fig.1 shows an example of an L- shell X-ray spectrum from a bismuth film irradiated by 12 MeV C^{3+} ions.

2.1 Determination of X-ray production cross sections

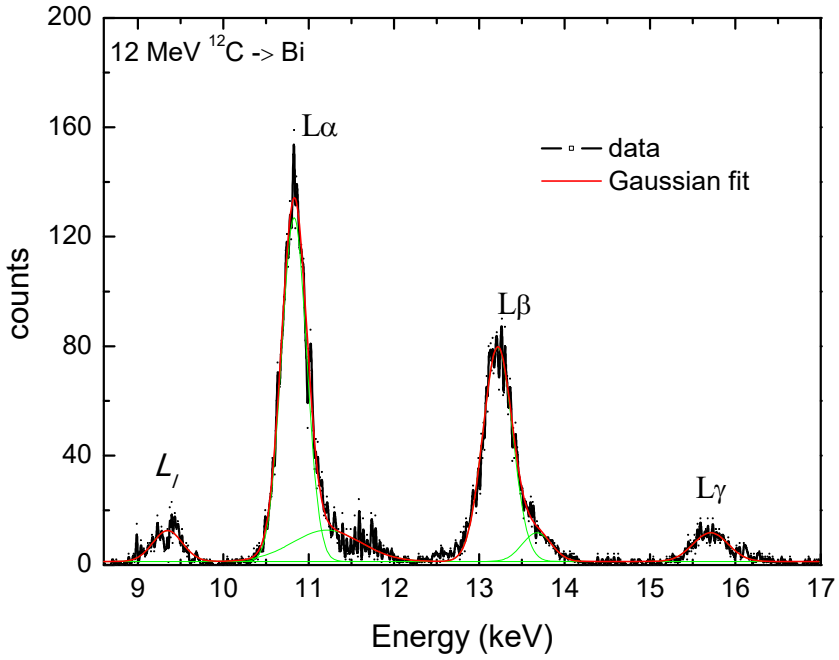

Fig. 1. Energy spectrum of Bi L-shell X-rays induced by 12 MeV carbon ions.

In this work, in order to evaluate heavy ion X-ray production cross sections, the X-ray yields from a target film as a result of the impingement of the heavy ion were compared to the X-ray yields from the same target due to 2 MeV protons under the same experimental conditions.

The formula used to calculate the heavy ion X-ray production cross section σ_X in the thin films in this work is given by (Msimanga et al., 2019; Yu and Chen, 2004):

$$\sigma_X = K\frac{N_X}{N_B}\cdot\frac{\sigma_B}{\varepsilon} \quad (1),$$

where K represents a constant obtained from a measurement of the X-ray yield due to 2 MeV protons;

$$K = \frac{A\Delta\Omega}{\beta N_A} = \frac{N_{B_p}}{N_{X_p}}\cdot\frac{\sigma_{X_p}}{\sigma_{B_p}}\cdot\varepsilon_p \quad (2),$$

In equations 1 and 2, N_X and N_B are the total counts under a given X-ray peak and backscattered ion peak respectively, ε is the energy dependent absolute detection efficiency of the X-ray detector, and σ_B is the backscattering cross sections for the incident heavy ion species. The molar mass of

the target is represented by A, $\Delta\Omega$ represents the solid angle subtended by the backscatter RBS detector, β is a factor that corrects for the absorption of X-rays emitted within the target film, and N_A is the Avogadro number. The nested subscript p refers to corresponding proton variables in both equations.

By introducing a new term, $f(E)$ in equation (1), the heavy ion X-ray production cross section can be rewritten as:

$$\sigma_X = \frac{N_X}{N_B} \cdot \frac{N_{B_p}}{N_{X_p}} \cdot \frac{\sigma_B}{\sigma_{B_p}} \cdot \sigma_{X_p} \cdot \frac{\varepsilon_p}{\varepsilon} \cdot f(E) \quad (3),$$

where all terms remain the same as defined by equation 1 and 2, and $f(E)$ is a factor that corrects for the energy loss of the incident ion through the target (see Eq. 6). In the case of 2 MeV protons, $f_p(E)$ is considered to be one as the energy loss of protons through the thin films is negligible.

2.1.1 Detector efficiency correction

For various methods of measurements and applications of elemental analysis that involve X-ray emission, it is recommended that the efficiency of the detector be precisely known over a range of energies to adequately cover all the characteristic X-ray energies involved in quantitative analysis. It has been established that the efficiency of a Si (Li) detector is strongly energy dependent, especially at low photon energies (≤ 5 keV). It is therefore important to have an accurate determination of the detector efficiency in order to make necessary corrections when comparing heavy ion induced X-ray production cross section measurement data and theoretical predictions. In order to determine the efficiency of the detector used in this work, measured K_α, K_β, L_α, L_β and L_γ X-ray intensities and ECPSSR calculated K- and L-shell X-ray production cross sections in ^{89}Y, ^{158}Gd and ^{209}Bi induced by 2 MeV protons were used. From equation 2, the formula used for the detector efficiency becomes:

$$\varepsilon_p = \frac{N_{X_p}}{N_{B_p}} \left(\frac{A\Delta\Omega}{N_A}\right) \frac{\sigma_{B_p}}{\sigma_{X_p}} \quad (4),$$

Fig. 2. Shows how the detector efficiency changes with photon energy. The solid line is a simple polynomial fit to the measurement data. As a result of the 10% estimated average uncertainty of ECPSSR calculated proton induced cross sections (Cohen et al., 2015), we assume that each data point has an uncertainty bar of ±10%. The uncertainty in the N_X and N_B integrals was below 2%

in all cases. The efficiency correction was then effected by multiplying the efficiency ratios $\left({}^{\varepsilon_p}/_{\varepsilon}\right)$ with the measured L-X-ray intensities as show in equation 3.

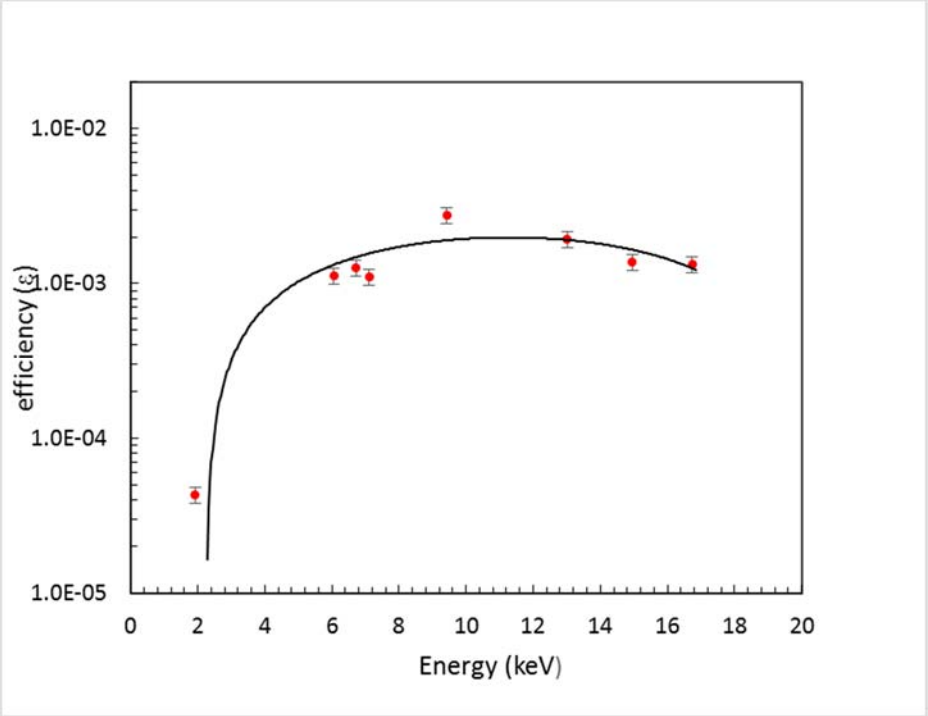

Fig. 2. Efficiency curve of the Si (Li) detector.

2.1.2 Energy loss correction

Considering the target thickness, as a projectile ion passes through, it loses energy and in the process X-rays emitted along its path are due to slightly lower ion energy than the incident energy. In order to ensure that the measured X-ray production cross sections correspond to the incident beam energy, it is imperative to ascertain that the energy loss by the incident ions is inconsequential when the incident energy is compared to the exit energy from the target.

Zucchiatti and co-workers (Zucchiatti et al., 2017), came up with a procedure for calculating the energy loss correction factor $F(E)$ in thin film targets and their formula can be given as:

$$\frac{1}{f(E)} = F(E) = \frac{\sigma_E}{\sigma_{E_i}} = \frac{1}{\Delta x.\sigma_{E_i}} \int_{E_f}^{E_i} \frac{\sigma_E(E)}{S(E)} dE \quad (5),$$

where Δx is the target thickness, E_i is the incident beam energy and E_f is the exit energy, σ_E is the measured cross section, σ_{E_i} is the cross section at the fixed incident energy E_i. The energy loss

correction factor is a function of the energy dependent X–ray production cross section and the ion stopping force in the target, implying that the target sample thickness and the nature of the ion play an important role in determining this factor. The integral in equation 6 can be calculated using Simpson's rule and is given as:

$$\int_{E_f}^{E_i} g(E)\,dE = \frac{E_{f-E_i}}{6}\left[g(E_i) + g(E_f) + 4g\left(\frac{E_i+E_f}{2}\right)\right] \quad (6),$$

where $g(E)$ is a polynomial function.

Energy loss correction factors were calculated and the correction effected for total L-shell X-ray production cross sections in the thin films using Equation (3).

3. RESULTS AND DISCUSSION

3.1 RBS data analysis

In order to extract film thickness from RBS data, simulation of the experimental RBS energy spectra was carried out using SIMNRA software (Mayer, 2014). The three target films used in this study were found to be (447 ± 21) x 10^{15} at/cm^2, (617 ± 28) x 10^{15} at/cm^2 and (522 ± 24) x 10^{15} atoms/cm^2 for yttrium, gadolinium and bismuth, respectively. These thickness values were converted to mass areal densities using the respective densities of gadolinium and bismuth. The quoted thickness uncertainty terms (of 4.6%) were estimated from the RBS measurement uncertainties arising mainly from the accuracy of SRIM stopping force data and the detector energy resolution.

3.2Multiple Ionization

L-shell multiple ionization due to heavy ion has been studied for decades (Berinde et al., 1987; Braziewiczt et al., 1991) and it has been established that, characteristic L-line X-ray energies shift to higher values and peaks are broadened due to MI of the target induced by heavy ion impact. The energy shift of the X-ray lines and the broadening of the peaks are caused by a reduced screening effect of the outer shell electrons of the target material and convoluted structure of many X-ray satellites respectively. While it has been affirmed that MI affects fluorescence yields only by a

small percentage (Berinde et al., 1987, Bogdanović et al., 1999), it is still important to study its effect on target materials especially when heavy ions are involved**.** Figure 3 below shows energy shifts in ^{158}Gd X-rays to higher energies due to 12 MeV C^{3+} ion bombardment relative to proton induced photon energies.

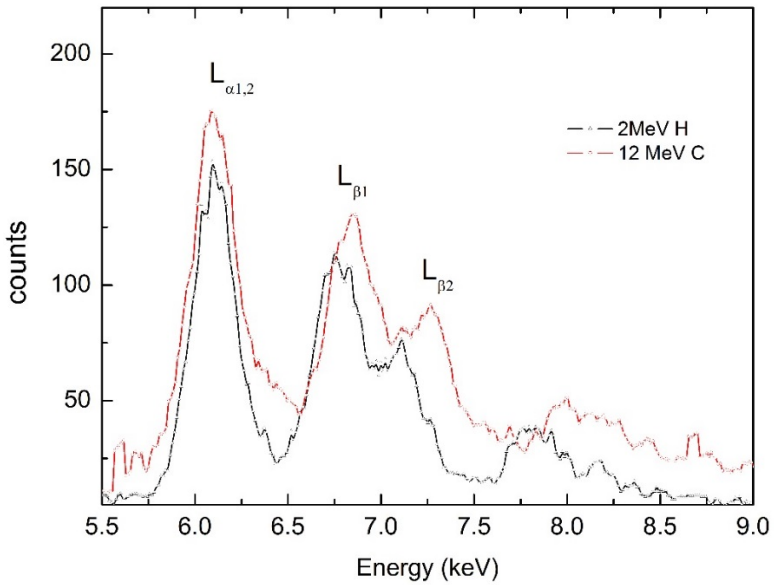

Fig. 3. Multiple ionization effect on gadolinium L-shell X-ray energies due to 1.0 MeV/u carbon projectiles.

Apart from the energy shift of the L X-rays which is caused by spectator vacancies in the M and higher shells, relative intensities of the L X-ray lines also give vital information about the degree of multiple ionization (Bogdanović et al., 1999). Changes in L-line intensity ratios, $L_{\alpha 1,2}/L_{\beta 2,15}$ in Gd and $L_{\beta 1}/L_{\gamma 1}$ in Bi were evaluated to determine the relative degree of ionisation of the M shell to the N shell (Ramakrishna, 2002). Table 1 shows these L-line intensity ratios in Gd and Bi due to C ions. The ratios were calculated taking into account the detection efficiency of each line energy and are quoted to an uncertainty of ±15 % in each case, obtained from uncertainties in the X-ray peak yields and the detector efficiency described earlier. The intensity ratios are compared to those of the presumably singly ionized target atom due to 2 MeV H^+ ions. In the case of Gd, the proton induced ratio is lower than the C-induced one, and the latter ratio is seen to increase with incident beam energy. The $L_{\alpha 1,2}$ and the $L_{\beta 2,15}$ X-ray energies are due to electron transitions from the $M_{4,5}$ to the L_3 subshell and from the $N_{4,5}$ to the L_3 subshell, respectively. The observed increase in the $L_{\alpha 1,2}/L_{\beta 2,15}$ ratio suggests that there are fewer electrons available for the $N_{4,5} \rightarrow L_3$ transition,

which implies a higher degree of ionization in the N shell compared to the M shell. For the Bi case $L_{\beta 1}/L_{\gamma 1}$ ratios for both proton and carbon projectiles are quite similar, which suggests the same kind of ion-target interactions as in the proton-target atom collisions. This implies that the carbon projectiles induce the same degree of multiple ionization in the Bi target atoms as the proton beam does. For the yttrium target there was no measurable shift in the energy of the dominant Lα-line.

Table 1. L line intensity ratios in ^{158}Gd and ^{209}Bi due to ^{12}C projectiles. Each data point is given with a ±15% uncertainty.

E (MeV)	Gd	Bi
	$L\alpha_{1,2}/ L_{\beta 2,15}$	$L_{\beta 1}/ L_{\gamma 1}$
6	2.2	4.0
8	2.3	3.9
10	2.5	5.3
12	2.6	4.5
2 MeV H^+	2.0	4.8

3.3 X-ray production cross sections

Results of the total L-X-ray production cross sections measurement in the three target elements studied here are summarized in Tables 2-4. Also included in the tables are cross sections from the ECPSSR and ECPSSR+UA model which were calculated using the ISICSoo code (Cipolla, 2007), and the ECPSSR+EC model which were calculated using the ERCS08 code (Horvat, 2009). For ^{89}Y the united atom (UA) electron capture corrections to the ECPSSR model are practically insignificant and so only the ECPSSR calculation is shown. The ISICSoo code uses fluorescence yields from the Krause database (Krause, 1979) and so for consistency the same database was used to convert theoretical ionization cross sections from the ERCS08 calculations to X-ray production cross sections. A quick calculation for 12 MeV C ions to check the effect of the choice of the fluorescence yields database (Krause 1979) *vs* (Campbell, 2009) on the theoretical cross sections revealed a difference of less than 5%.

The uncertainty evaluation in the measured cross sections is based on the physical variables in Equation 3. The main contributors to uncertainty are the uncertainties in the detection efficiency,

estimated to be 10%, and in the proton induced X-ray ionisation cross sections for the L-lines. Cohen and co-workers (Cohen et al., 2015) cite a 5% -15 % uncertainty range for proton induced cross sections. Since there are no specific uncertainty values for individual elements, in this work we have taken 10% as our estimate of the average uncertainty in these cross sections. The other contributions to the overall uncertainty come from the statistical uncertainty in the X–ray and backscattered particle yields. For Gd these ranged from 0.8% to 2% and 0.1% to 0.7%, respectively. For Bi the X-ray yield uncertainties varied from 1.2% to 4.2 % and the backscattered particle count uncertainty ranged from 0.1% to 0.5 %. In the yttrium measurements the statistical uncertainties were generally below 0.1%. Combining the ε, N_X, N_B and σ_{XP} uncertainty estimates in quadrature yields an upper estimate of about 15% uncertainty in our measured cross sections.

Table 2: Experimental (σ_{expt}) L-shell X-ray production cross sections in ^{89}Y due to 4 MeV-12 MeV C ions together with calculated values of the ECPSSR model.

E (MeV)	**σ_{expt} (kb)**	**ECPSSR (kb)**
4	0.55 ± 0.08	0.65
6	1.8 ± 0.3	2.3
8	3.4 ± 0.5	5.2
10	6.1 ± 0.9	9.1
12	9.2 ± 1.4	13.6

Table 3: Experimental (σ_{expt}) X-ray production cross sections in ^{158}Gd due to 6 MeV-12 MeV C ions together with calculated values of ECPSSR, ECPSSR + EC and ECPSSR + UA models.

E (MeV)	**σ_{expt} (b)**	**ECPSSR (b)**	**ECPSSR+EC (b)**	**ECPSSR+UA (b)**
6	99 ± 15	50	92	65
8	205 ± 30	129	238	155
10	328 ± 50	260	479	287
12	388 ± 60	444	601	467

Table 4: Experimental (σ_{expt}) X-ray production cross sections in ^{209}Bi due to 4 MeV-12 MeV C ions together with calculated values of ECPSSR, ECPSSR + EC and ECPSSR + UA models.

E (MeV)	σ_{expt} (b)	ECPSSR (b)	ECPSSR+EC (b)	ECPSSR+UA (b)
4	0.32 ± 0.05	1.06	1.11	1.09
6	3.7 ± 0.6	6.23	6.58	6.44
8	10.4 ± 1.5	18.1	19.3	18.8
10	18.3 ± 2.7	38.3	41.0	39.7
12	30.3 ± 4.5	67.3	72.6	69.7

Measured L-shell X-ray production cross sections in ^{89}Y, ^{158}Gd and ^{209}Bi induced by C ions are shown in Fig. 4, in comparison to ECPSSR, ECPSSR+UA and ECPSSR+EC predictions. Also included in Fig. 4 are data from Mehta *et al* (Mehta et al., 1995) for ^{89}Y and ^{158}Gd, and from Lugo-Licona *et al* for ^{158}Gd (Lugo-Licon, 2004). In all cases theoretical predictions show the same trend as the experimental data. For yttrium deviation between our data and Mehta *et al*'s is about 20%. The ECPSSR theory overestimates our measurements by up to 50%. For the gadolinium case, the largest disagreement between our data and Mehta *et al*'s is about 30 %, at 8 MeV. Data from Lugo-Lucona and co-workers is roughly mid-way ours and that from Mehta's group. We note that while The ECPSSR theory describes the literature data quite well, our data is better described by the ECPSSR+EC modification, particularly in the lower energy region. Indeed the ECPSSR theory underestimates Mehta and co-workers data by close to 30% at 6 MeV. However as energy increases towards 1.0 MeV/u the direct ionisation ECPSSR model appears to describe the ion-target interaction fairly accurately, without the additional modifications, and both data sets attest to that. For the bismuth case, the theoretical predictions are all in agreement but they overestimate our data by an almost constant factor of two. The agreement between the three theoretical calculations implies that the additional modifications by the UA and EC models beyond direct ionization are insignificant for this ion-target pair at these beam energies.

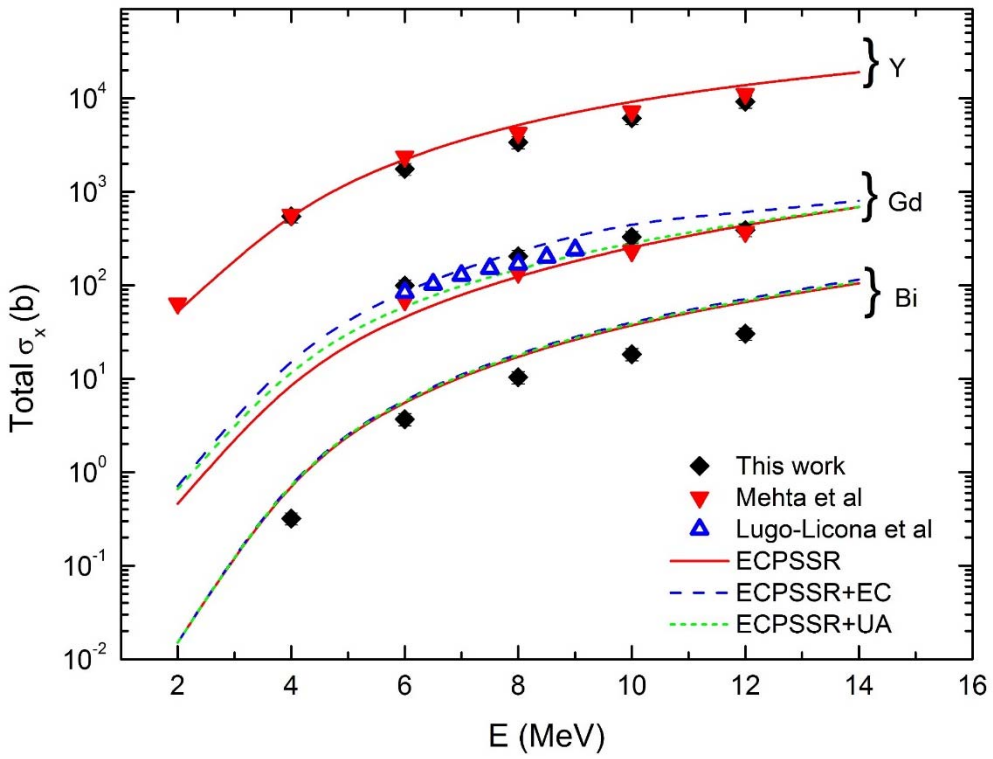

Fig. 4. Experimental and theoretical X-ray production cross sections in ^{89}Y, ^{158}Gd and ^{209}Bi induced by carbon ions of 4 MeV-12 MeV.

No carbon-bismuth data could be found in the literature over this same energy range. To get a more universal comparison of our data with literature data showing other ion-target combinations, in addition to our C-Gd and and C-Bi data, we show in Fig. 5 X-ray production cross sections in: gadolinium due to 0.5 MeV/u – 0.75 MeV/u ^{12}C ions (Lugo-Licona et al., 2004), 0.5 MeV/u – 0.75 MeV/u ^{14}N ions (Murillo et al., 2016) and 0.58 MeV/u - 0.75 MeV/u ^{9}Be ions (Miranda et al., 2018); and in bismuth due to 0.4 MeV/u – 2.0 MeV/u ^{32}S ions (Fijał-Kirejczyk et al., 2008), 0.8 MeV/u – 1.6 MeV/u ^{16}O ions(Gorlachev et al., 2016) and 0.7 MeV/u – 1.5 MeV/u ^{1}H ions (Goudarzi et al., 2006). The ^{158}Gd cross sections data due to the three ^{9}Be, ^{12}C and ^{14}N projectile species is expectedly lumped together because of the closeness of the Z-values of the projectiles. For ^{209}Bi the cross sections are much more spread out because of the larger Z-range of the projectile species (1-16). In all instances though the cross sections, on average, increase in the same manner with projectile velocity.

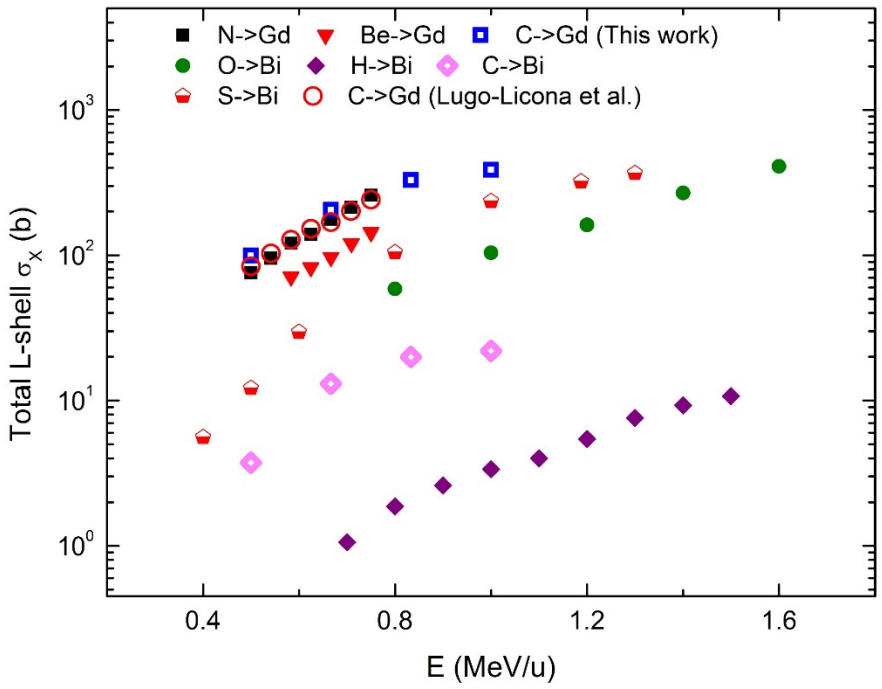

Fig. 5. Comparison of the C-Gd and C-Bi cross sections measured in this work with literature data over similar energy ranges (*refer to text for the literature data references*).

4. **CONCLUSION**

Total L shell X production cross sections for ^{89}Y, ^{158}Gd and ^{209}Bi induced by carbon ions in the energy range of 4 MeV to 12 MeV have been measured to add to the sparse database of heavy ion induced cross sections. Comparisons of our yttrium and gadolinium data with literature data show reasonable agreement, within experimental uncertainty limits. For bismuth, the energy variation trend of our data is similar to that of other projectile species within the same energy range. When compared with ECPSSR, ECPSSR+EC and ECPSSR+UA models predictions, our data show fairly good, though energy dependent agreement with the different models for yttrium and gadolinium cross sections. For bismuth, all three models overestimate data by an almost constant factor of two.

REFERENCES

Berinde, A., Ciortea, C., Enulescu, A., Fluerasu, D., Hock, G., Piticu, I., Sarkadi, L., Sulik, B., Zoran, V., 1987. On the L-M-N multiple ionisation in heavy elements. J. Phys. B At. Mol. Phys. 20, L481–L486. https://doi.org/10.1088/0022-3700/20/15/005

Bogdanović, I., Tadić, T., Jakšić, M., Halabuka, Z., Trautmann, D., 1999. L-shell ionization of Cd, Sb, Te, Ba, La, Eu, Tb and Yb by16O ions in the energy range from 0.19 to 0.75 MeV u-1. Nucl. Instrum Methods Phys. Res. B 150, 16–26. https://doi.org/10.1016/S0168-583X(98)00925-2

Brandt, W., Lapicki, G., 1981. Energy-loss effect in inner-shell Coulomb ionization by heavy charged particles. Phys. Rev. A 23, 1717–1729. https://doi.org/10.1103/PhysRevA.23.1717

Brandt, W., Lapicki, G., 1979. L-shell Coulomb ionization by heavy charged particles. Phys. Rev. A 20, 465–480. https://doi.org/10.1103/PhysRevA.20.465

Bransden, B.H., McDowell, M.R.C., Mansky, E.J., 1993. Charge Exchange and the Theory of Ion–Atom Collisions. Phys. Today 40, 24. https://doi.org/10.1063/1.2809074

Braziewiczt, E., Braziewiczt, J., Czyzewskif, T., Glowacka$, L., Jask6laf, M., Kauers, T., Kobzevll, A.P., Pajekf, M., Trautmanns, D., 1991. L-subshell ionization of rare earth elements by light ion bombardment. J. Phys. B At. Mol. Opt. Phys. J. Phys. E At. Mol. Opt. Phys 24, 1669–1682. https://doi.org/http://dx.doi.org/10.1088/0953-4075/24/7/020

Campbell, J.L., 2009. Fluorescence yields and Coster – Kronig probabilities for the atomic L subshells . Part II : The L1 subshell revisited. At. Data Nucl. Data Tables 95, 115–125. https://doi.org/10.1016/j.adt.2008.08.002

Cipolla, S.J., 2007. The united atom approximation option in the ISICS program to calculate K-, L- and M-shell cross sections from PWBA and ECPSSR theory. Nucl. Instrum Methods Phys. Res.B 261, 142–144. https://doi.org/10.1016/J.NIMB.2007.03.057

Cohen, D.D., 1990. K and L shell X-ray cross sections for use in PIXE analysis systems. Nucl. Instrum. Methods Phys. Res. B 49, 1–9. https://doi.org/10.1016/0168-583X(90)90206-A

Cohen, D.D., Crawford, J., Siegele, R., 2015. K, L, and M shell datasets for PIXE spectrum fitting and analysis. Nucl. Instrum Methods Phys. Res. B 363, 7–18. https://doi.org/10.1016/j.nimb.2015.08.012

Fijał-Kirejczyk, I., Jaskóła, M., Korman, A., Banaś, D., Braziewicz, J., Choiński, J., Majewska, U., Pajek, M., Kretchmer, W., Lapicki, G., Mukoyama, T., Trautmann, D., 2008. L-subshell ionization of heavy elements by S ions with energy of 0.4-3.8 MeV/amu. Nucl. Instrum Methods Phys. Res. Sect. B 266, 2255–2258. https://doi.org/10.1016/j.nimb.2008.03.047

Gorlachev, I., Gluchshenko, N., Ivanov, I., Kireyev, A., Kozin, S., Kurakhmedov, A., Platov, A., Zdorovets, M., 2016. K-, L- and M-shell X-ray productions induced by oxygen ions in the 0.8–1.6 MeV/amu range. Nucl. Instrum Methods Phys. Res. B 381, 34–38. https://doi.org/10.1016/j.nimb.2016.05.020

Goudarzi, M., Shokouhi, F., Lamehi-Rachti, M., Oliaiy, P., 2006. L-subshell and total M-shell X-

ray production cross sections of Ta, W, Pt, Au, Pb and Bi by 0.7-2.4 MeV protons. Nucl. Instruments Methods Phys. Res. B 247, 217–222. https://doi.org/10.1016/j.nimb.2006.03.001

Govil, I.M., 2001. Proton induced X-ray emission - A tool for non-destructive trace element analysis. Curr. Sci. 80, 1542–1549. https://doi.org/10.1016/0029-554X(74)90831-3

Horvat, V., 2009. ERCS08: A FORTRAN program equipped with a Windows graphics user interface that calculates ECPSSR cross sections for the removal of atomic electrons. Comput. Phys. Commun. 180, 995–1003. https://doi.org/10.1016/j.cpc.2008.12.034

Kumar, S., Singh, U., Oswal, M., Singh, G., Singh, N., Mehta, D., Nandi, T., Lapicki, G., 2017. L shell x ray production in high-Z elements using 4–6 MeV/u fluorine ions. Nucl. Instrum Methods Phys. Res. Sect. B 395, 39–51. https://doi.org/10.1016/j.nimb.2017.01.044

Lapicki, G. McDaniel, F.., 1980. Electron capture from E shells by fully stripped iona. Phy. Rev. 22, 1896–1905. https://doi.org/https://doi.org/10.1103/PhysRevA.22.1896

Lapicki, G., 2002. The status of theoretical L-subshell ionization cross sections for protons. Nucl. Instrum Methods Phys. Res. B 189, 8–20. https://doi.org/10.1016/S0168-583X(01)00987-9

Lugo-Licona, M., Miranda, J., Romo-Kröger, C.M., 2004. L-shell X-ray production cross section measured by heavy ion impact on selected rare earth elements. J. Radioanal. Nucl. Chem. Vol. 262, 391–401. https://doi.org/10.1023/B:JRNC.0000046768.47058.75

Mayer, M., 2014. Improved physics in SIMNRA 7. Nucl. Instrum Methods Phys. Res. B 332, 176–180. https://doi.org/10.1016/j.nimb.2014.02.056

Mehta, R., Sun, H.L., Marble, D.K., Duggant, J.L., McDaniel, F.D., Lapicki, G., 1995. L-shell X-ray production by 2-12 MeV carbon ions in fifteen selected elements from copper to lead. J. Phys. B At. Mol. Opt. Phys. 28, 1187–1189.

Miranda, J., De Lucio, O.G., Lugo-Licona, M.F., 2007. X-ray production induced by heavy ion impact: Challenges and possible uses. Rev. Mex. Fis. 53, 29–32.

Miranda, J., Murillo, G., Méndez, B., Villaseñor, P., 2018. Measurement of L X-ray production cross sections of Ce, Nd, Sm, Eu, Gd, and Dy by impact of 9Be2+ ions with energies in the interval 5.25 MeV to 6.75 MeV. Nucl. Instrum Methods Phys. Res. Sect. B 434, 93–96. https://doi.org/10.1016/j.nimb.2018.08.032

Msimanga, M., Pineda-Vargas, C.A., Madhuku, M., 2019. L-shell X-ray production cross sections in metal oxide thin films due to 12C, 16O and 28Si ion beams at MeV SIMS energies. Nucl. Instrum Methods Phys. Res. B 440, 186–190. https://doi.org/10.1016/J.NIMB.2018.08.050

Msimanga, M., Pineda-Vargas, C.A., Madhuku, M., 2016. K-shell X-ray production cross sections in Ti by 0.3-1.0 MeV/u12C and28Si ions for heavy ion PIXE. Nucl. Instrum Methods Phys. Res. B 380, 90–93. https://doi.org/10.1016/j.nimb.2016.05.012

Murillo, G., Miranda, J., Méndez, B., Villaseñor, P., 2016. L-shell X-ray production cross sections of Ce, Nd, Sm, Eu, Gd, and Dy by impact of 14N2+ ions with energies between 7.0 MeV and 10.5 MeV. Nucl. Instrum Methods Phys. Res. B 383, 89–92. https://doi.org/10.1016/j.nimb.2016.06.014

Orlić, I., Osipowicz, T., Sow, C.H., 1998. L X-ray production cross sections of medium Z elements by4He ion impact. Nucl. Instrum Methods Phys. Res. B 136–138, 184–188. https://doi.org/10.1016/S0168-583X(97)00675-7

Paul, H., Muhr, J., 1986. Review of experimental cross sections for k-shell ionization by light ions. Phys. Rep. 135, 47–97. https://doi.org/https://dx.doi.org/10.1016/0370-1573(86)90149-3

Prieto, J.E., Zucchiatti, A., Galán, P., Prieto, P., 2017. Cross sections of X-ray production induced by C and Si ions with energies up to 1 MeV/u on Ti, Fe, Zn, Nb, Ru and Ta. Nucl. Instrum Methods Phys. Res. B 406, 167–172. https://doi.org/10.1016/J.NIMB.2017.01.047

Reis, M.A., Jesus, A.P., 1996. Semiempirical Approximation to Cross Sections forLX-ray Production by Proton Impact. At. Data Nucl. Data Tables 63, 1–55. https://doi.org/10.1006/ADND.1996.0008

Ryan, C.G., 2011. PIXE and the nuclear microprobe: Tools for quantitative imaging of complex natural materials. Nucl. Instrum Methods Phys. Res. B 269, 2151–2162. https://doi.org/10.1016/j.nimb.2011.02.046

Sarkadi, L., Mukoyama, T., 1991. Systematic study of helium-induced L shell ionization cross sections. Nucl. Instrum Methods Phys. Res. B 61, 167–17. https://doi.org/10.1016/0168-583X(91)95456-N

Scafes, A.C., Ciortea, C., Dumitriu, D.E., Enulescu, A., Fluerasu, D., Gugiu, M.M., Pena, M.D., Pentia, M., Piticu, I., 2014. K-shell ionization cross sections of Ti , Cr , Ni , Cu , and Zr in collisions with 16 O ions at Mev / u energies. Rom. Reports Physics, 66, 455–471.

Schmelmer, O., Dollinger, G., Datzmann, G., Hauptner, A., Körner, H.J., Maier-Komor, P., Reichart, P., 2001. Particle-induced X-ray emission using high energy ions with respect to microprobe application. Nucl. Instrum Methods Phys. Res. B 179, 469–479. https://doi.org/10.1016/S0168-583X(01)00608-5

Tadić, T., Bogdanović Radović, I., Siketić, Z., Cosic, D.D., Skukan, N., Jakšić, M., Matsuo, J., 2014. Development of a TOF SIMS setup at the Zagreb heavy ion microbeam facility. Nucl. Instrum Methods Phys. Res. B 332, 234–237. https://doi.org/10.1016/J.NIMB.2014.02.068

Yu, Y.C., Chen, K.M., 2004. M X-ray production in Nd, Gd, Ho and Lu by 1–6 MeV lithium ions. Nucl. Instrum Methods Phys. Res. B 219–220, 284–288. https://doi.org/10.1016/J.NIMB.2004.01.069

Zucchiatti, A., Galán, P., Emilio, J., 2017. Nucl Instrum and Methods in Phys Res B A procedure to correct for target thickness effects in heavy-ion PIXE at MeV energies. Nucl. Inst. Methods Phys. Res. B 407, 1–4. https://doi.org/10.1016/j.nimb.2017.05.022